

RSC Advances



This is an *Accepted Manuscript*, which has been through the Royal Society of Chemistry peer review process and has been accepted for publication.

Accepted Manuscripts are published online shortly after acceptance, before technical editing, formatting and proof reading. Using this free service, authors can make their results available to the community, in citable form, before we publish the edited article. This *Accepted Manuscript* will be replaced by the edited, formatted and paginated article as soon as this is available.

You can find more information about *Accepted Manuscripts* in the [Information for Authors](#).

Please note that technical editing may introduce minor changes to the text and/or graphics, which may alter content. The journal's standard [Terms & Conditions](#) and the [Ethical guidelines](#) still apply. In no event shall the Royal Society of Chemistry be held responsible for any errors or omissions in this *Accepted Manuscript* or any consequences arising from the use of any information it contains.

Cite this: DOI: 10.1039/c0xx00000x

www.rsc.org/xxxxxx

ARTICLE TYPE

Density functional study on 3d metal/graphene for removing CO from H₂ feed gas in hydrogen fuel cells

Kai Li,^a Yang Li,^b Hao Tang,^{*b} Menggai Jiao,^a Ying Wang^{*a} and Zhijian Wu^{*a}

Received (in XXX, XXX) Xth XXXXXXXXX 20XX, Accepted Xth XXXXXXXXX 20XX

DOI: 10.1039/b000000x

Metal/graphene has been used as a filter membrane exterior to the hydrogen fuel cell to prevent CO poisoning. Therefore, removing CO from H₂ feed gas is important for efficient use of anode catalyst and would increase the lifetime of the fuel cells. In this work, the adsorptions of CO and H₂ on metal/perfect-graphene (M/G_p) and metal/defect-graphene (M/G_d) (M= Sc - Zn) are investigated by using the density functional theory. Our results indicated that the defect site in graphene enhances the stability of metal on the graphene compared with perfect graphene. For gas molecule adsorption, however, CO and H₂ adsorption is more weakly on defect graphene compared with perfect one, due to the more localized metal d electrons in the former case. For both defect and perfect graphene, Fe/G_{p(d)}, Co/G_{p(d)} and Ni/G_{p(d)} are more effective in separating CO from H₂ feed gas, in particular for the perfect graphene. Orbital analysis suggested that d_{yz} and/or d_{xz} orbitals of metal atoms play a major role in CO and H₂ adsorption.

1. Introduction

Current energy productions are mainly from the unsustainable resource such as fossil fuels. However, the depleted resources and environmental pollution of the fossil fuels limited their use. Fuel cell is electrochemical cell that converts chemical energy into electrical energy which is one of attractive replacements for fossil fuels.^{1,2} Currently, platinum is widely utilized as anode electrocatalyst due to its high catalytic activity toward the redox reactions of H₂ and O₂.³ The hydrogen for the anode reaction is mainly produced by steam reforming of methane. This results in hydrogen feed gas containing an appreciable amount of CO (0.5~2%), and it is known that CO level as little as 20 ppm would poison the anode catalyst by blocking hydrogen adsorption sites.⁴ Therefore, the presence of CO is one of the obstacles and is particularly challenging for the development of fuel cells. In order to avoid catastrophic poisoning of the fuel cell anode, CO concentration needs to be removed or at least reduced.

To improve the CO tolerance, many electrode materials are investigated. It is found that the presence of a second metal changes the CO chemisorptions by modifying the Pt electronic properties and promotes the oxidation of CO to CO₂.⁵⁻⁷ Thus, many binary PtM alloys have been investigated, such as PtRu, PtRh and PtPd.⁸⁻¹⁶ The most promising alloy is PtRu catalyst due to more effectively promoting the electro-oxidation and higher CO tolerance,¹¹⁻¹⁶ while the high cost of Ru and Pt limited its widespread application. After that, several Pt-based electrodes by alloying Pt with a second non-precious metal (PtFe, PtCo, PtNi, PtSn and PtW etc.) were also found to have excellent CO tolerance and oxidation reaction.¹⁶⁻²⁴ Although the catalytic life is lengthened in these Pt alloys, CO poison still exists. On the other hand, some other techniques have been investigated to improve

the CO tolerance in fuel cell, such as air bleeds (2CO+O₂→2CO₂) and water-gas shift reaction (WGS, CO+H₂O↔CO₂+H₂).²⁵⁻³¹ The difficulty of air bleeds is to maintain high reaction rate and selectivity for oxidizing CO rather than H₂.²⁵⁻²⁷ while for WGS, the reaction shows low activities at low temperatures.²⁸⁻³¹ Thus, an ideal method would be to remove CO before H₂ reaches the catalyst.

The mechanism for CO poison has also been studied theoretically. In a practical catalytic process, the Pt catalyst is usually fully covered by H atoms and/or CO molecules and Pt catalytic activity is coverage dependent.^{32,33} The dissociative energy of hydrogen on Pt(111) is between 0.70 and 0.83 eV,³⁴⁻³⁶ while CO adsorption energy on Pt(111) is between 1.49 and 1.8 eV.^{37,38} This means that CO molecule would bind more strongly on Pt catalysts to block the available sites for dissociating H atoms. Furthermore, it was found that each CO molecule could roughly exclude two H atoms on the Pt₆ cluster and the poisoning effect was partially due to the loss of Pt (5d) electrons upon CO adsorption.³⁹ It is also found that the enhancement for CO tolerance could be achieved by reducing its adsorption, facilitating CO oxidation or removing CO from H₂ feed gas, while the later one seems more effective in preventing catalyst from CO poisoning by allowing almost pure H₂ reaching catalyst. Recently, metal deposition on carbon based materials are widely investigated and used in fuel cells due to the high activity.^{10-14,17-19} Theoretical study indicated that metal/graphene (Ni/G, Pt/G and IrAu/G) bound CO strongly while having minimal interaction with H₂, which were potential materials to remove CO from the H₂ feed gas.⁴⁰ In that work, however, only the interaction between perfect graphene and transition metals is considered.⁴⁰ It is known that defects occur frequently in graphene synthesis. Therefore, to find more applicable systems with the capability of

capturing CO from H₂ feed gas, the non-precious metals M (M=Sc-Zn) adsorbed on both perfect and single point defect graphene are examined. The density functional theory method was used to study CO and H₂ binding behavior on different metals.

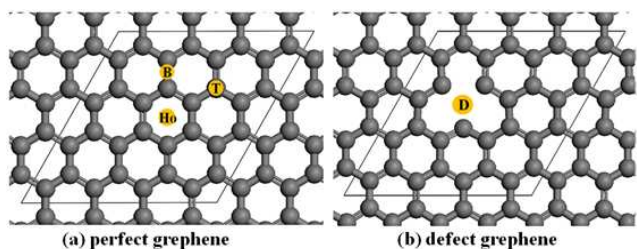


Fig. 1 (Color online) The possible adsorption sites on perfect and defect graphene, respectively. B, T, Ho and D denote the bridge, top, hollow and defect sites, respectively.

10

2. Computational Details

2.1. Method

The calculations were performed using Vienna ab-initio simulation package (VASP).⁴¹⁻⁴⁴ The interactions between valence electrons and ion cores were treated by Blöchl's all-electron-like projector augmented wave (PAW) method.^{45,46} The exchange-correlation functional was the generalized gradient approximation with the Perdew-Burke-Ernzerhof, known as GGA-PBE.⁴⁷ The wave functions at each k-point were expanded with a plane wave basis set and a kinetic cutoff energy up to 400 eV. The electron occupancies were determined according to Fermi scheme with an energy smearing of 0.1 eV. Brillouin zone integration was approximated by a sum over special selected k-points using the Monkhorst-Pack method⁴⁸ and they were set to 3×3×1. Geometries were fully optimized until the energy was converged to 1.0 × 10⁻⁶ eV/atom and the force was converged to 0.01 eV/Å. Because of the existence of the magnetic atom, spin polarization was considered in all calculations. Since H₂ adsorption would be weak physisorption, a semiempirical DFT-D2 force-field approach,^{49,50} which includes the van der Waals interaction, is employed in our calculations.

2.2. Model

A 4×4 perfect graphene surface (G_p, including 32 C atoms) and a single point defect graphene (G_d, including 31 C atoms) are set as the planar unit cell (9.84 Å×9.84 Å×12 Å) for periodic calculation in this work. The structures of G_p and G_d are shown in Fig. 1a and b, respectively, as well as the possible adsorption sites of metal atom. The geometries are fully optimized after the metal atom adsorbed and the most stable structures are shown in Fig. S1 (for G_p) and S2 (for G_d) in Supporting Information.

The adsorption energy of the metal atoms on the graphene is calculated by equation (1) in the following, while the adsorption energy of gas molecule (CO or H₂) on the metal/graphene system (ΔE_g) was calculated by equation (2). The difference between the adsorption energies of CO and H₂ is calculated by ΔE_{diff} in equation (3). The larger the $|\Delta E_{diff}|$, the more effective to separate CO from H₂ feed gas.

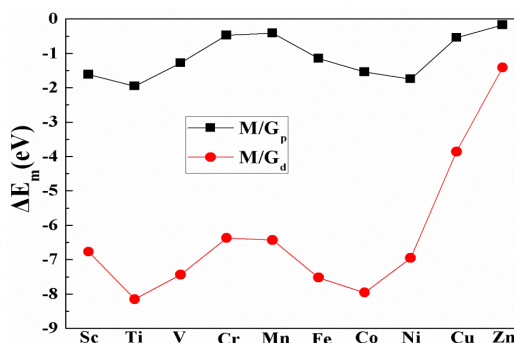


Fig. 2 (Color online) The adsorption energies of metal atoms (Sc-Zn) on perfect graphene (black line) and defect graphene (red line), respectively.

$$\Delta E_m = E_{metal/graphene} - E_{graphene} - E_{metal} \quad (1)$$

$$\Delta E_g = E_{(metal+gas)/graphene} - E_{metal/graphene} - E_{gas} \quad (2)$$

$$\Delta E_{diff} = \Delta E_{CO} - \Delta E_{H_2} \quad (3)$$

where the $E_{graphene}$, $E_{metal/graphene}$ and $E_{(metal+gas)/graphene}$ denote the total energies of isolated graphene, metal/graphene and H₂/CO adsorption on metal/graphene, respectively. The E_{metal} and E_{gas} denote the total energies of single metal atom and isolated gas, respectively, which are calculated by setting the single metal atom or gas in a box of 12 Å×12 Å×12 Å. The negative ΔE indicates exothermic chemisorption, and positive value suggests endothermic chemisorption.

3. Results and discussion

3.1. The stability of 3d transition metals (from Sc to Zn) adsorption on graphene

For perfect graphene (G_p), all the possible metal adsorption sites, i.e. bridge (B), hollow (Ho) and top (T) sites are examined (Fig. 1). It is found that Ho site is energetically the most stable site for most of the 3d metal atoms adsorption (except Cu), which is in agreement with the previous theoretical study.⁵¹ For Cu, the most stable site is at B site.

For perfect graphene, the adsorption energy is the largest for Ti/G_p with $\Delta E_m = -1.95$ eV, followed by Ni/G_p with $\Delta E_m = -1.75$ eV (Fig. 2). For Cr, Mn, Cu and Zn with either half filled d⁵ or fully filled d¹⁰ orbitals, the adsorption energy is relatively high, in particular for Zn/G_p with $\Delta E_m = -0.18$ eV. This suggests that the interaction between M and G_p will be influenced by the number of d electrons of the metal atom.⁴⁰

For defect graphene, the calculated adsorption energy shows similar trend to the perfect one. However, the absolute values of the adsorption energy of metal atoms increases significantly (Fig. 2) due to the charge transfer mechanism,^{52,53} suggesting that the defect on graphene can enhance the adsorption of metal atoms. This can be explained that the dangling bonds at defect site are saturated by the metal atom and it further induces the strong interaction between metal atom and the nearby C atoms. This is consistent to the previous observations.^{52,53} The largest adsorption energy is found for Ti/G_d ($\Delta E_m = -8.15$ eV), followed by Co/G_d ($\Delta E_m = -7.96$ eV). Since Zn is the least stable in both perfect and defect graphene, it is excluded in the following CO/H₂ separation

study.

Table 1 The average bond distances (\AA) between the adsorbed molecules and metal atoms.

	perfect graphene		defect graphene	
	CO	H ₂	CO	H ₂
Sc	2.12	2.05	2.37	2.59
Ti	2.04	1.99	2.23	2.34
V	1.99	1.89	2.09	2.07
Cr	1.93	1.83	2.03	1.99
Mn	1.82	1.66	1.90	1.75
Fe	1.78	1.64	1.88	1.75
Co	1.75	1.56	1.84	1.82
Ni	1.72	1.54	1.85	1.81
Cu	1.79	1.59	1.84	1.72

3.2. The adsorption of CO and H₂ on M/G_p

For adsorption of H₂ and CO on M/G_p (M= Sc - Cu), the optimized geometry structures are shown in Supporting Information (Fig. S3 and S4). Our calculations indicated that the average distance between the metal atom and CO molecule (Table 1) decreases from Sc (2.12 \AA) to Ni (1.72 \AA), with slight increase for Cu/G_p (1.79 \AA). Similar result is observed for H₂ adsorption, i.e., the average distance between M and H₂ decreases from Sc (2.05 \AA) to Ni (1.54 \AA), with slight increase for Cu (1.59 \AA). For CO adsorption, the energies increase from Sc (-1.17 eV) to Ni (-2.90 eV), with dramatic decrease for Cu/G_p (-1.59 eV) compared with Ni/G_p (Fig. 3a). Thus, Ni/G_p has the strongest adsorption for CO with a value of -2.90 eV, followed by Co/G_p (-2.69 eV) and Fe/G_p (-2.56 eV). Similar to the results of CO adsorption, more stable H₂ adsorption are found for Ni/G_p, Co/G_p, and Fe/G_p with values of -1.40, -1.24 and -1.09 eV, respectively. Furthermore, the energy difference between ΔE_{CO} and ΔE_{H_2} , i.e., ΔE_{diff} is the largest for Ni/G_p with a value of -1.50 eV, followed by Fe/G_p, Co/G_p and Mn/G_p with values of -1.47, -1.45, and -1.45 eV, respectively. Since Mn/G_p is relatively unstable ($\Delta E_m = -0.41$ eV) compared with the other three systems ($\Delta E_m = -1.15$, -1.54 and -1.75 eV for Fe/G_p, Co/G_p and Ni/G_p, respectively), this means that M/G_p (M= Fe, Co and Ni) systems are supposed to be the promising materials to remove CO from the H₂ feed gas, in particular for Ni/G_p.

3.3. The adsorption of CO and H₂ on M/G_d

The adsorption geometries of CO and H₂ on M/G_d are shown in Supporting Information (Fig. S5 and S6). For CO adsorption, the average distance between metal atom and carbon decreases from 2.37 \AA (Sc) to 1.84 \AA (Cu) (Table 1). For H₂ adsorption, the average distance between metal atom and H₂ decreases from Sc (2.59 \AA) to Cu (1.72 \AA) in general, with slight increase for Co (1.82 \AA) and Ni (1.81 \AA) compared with Mn (1.75 \AA) and Fe (1.75 \AA). For the adsorption energy, it is seen that Fe/G_d is the most stable system for H₂ (-0.54 eV) and CO (-1.54 eV) adsorption, followed by Co/G_d system (-0.26 and -1.34 eV for H₂ and CO, respectively) (Fig. 3b). Furthermore, the gas molecule adsorption on M/G_d (Fig. 3b) is weaker than that on M/G_p (Fig. 3a), which is consistent with the longer metal-gas molecule distances for the former. This revealed that the defect on graphene will weaken the ability of metal atom adsorbing CO and H₂. This can be explained by the change of orbital occupancy after CO and

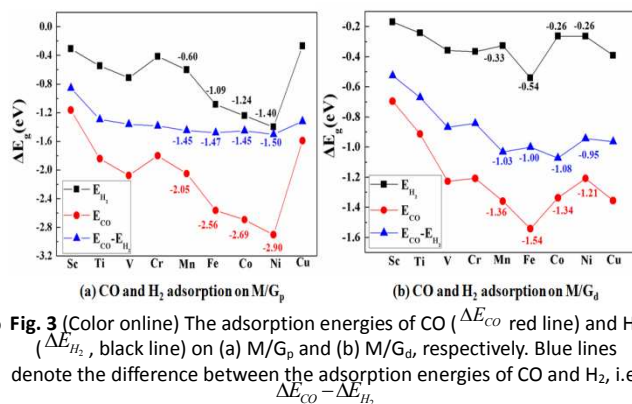


Fig. 3 (Color online) The adsorption energies of CO (ΔE_{CO} red line) and H₂ (ΔE_{H_2} , black line) on (a) M/G_p and (b) M/G_d, respectively. Blue lines denote the difference between the adsorption energies of CO and H₂, i.e. $\Delta E_{diff} = \Delta E_{CO} - \Delta E_{H_2}$.

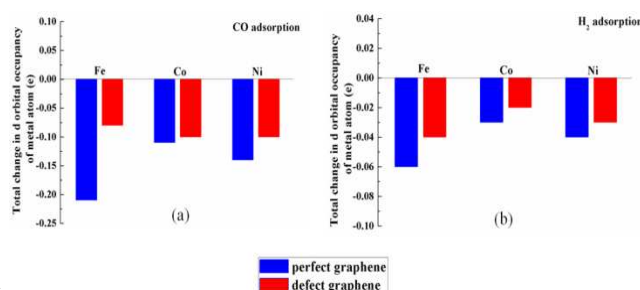


Fig. 4 (Color online) The total change in d orbital occupancy of Fe, Co and Ni when the CO and H₂ is adsorbed with reference to the isolated M/G_{p(d)}.

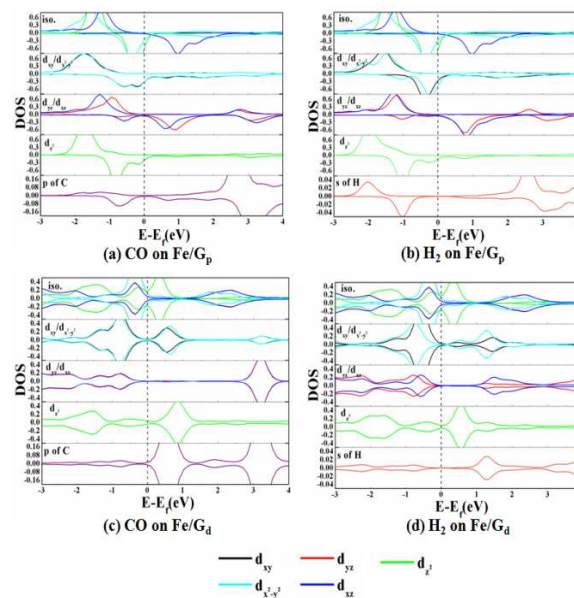


Fig. 5 (Color online) The partial density of states (DOS) of CO and H₂ adsorption on Fe/G_p and Fe/G_d. iso. represents the isolated M/G_p without CO or H₂ adsorption. The dotted line denotes the Fermi level.

H₂ are adsorbed. Previous theoretical study has found that orbitals of metal atoms play a major role in molecule adsorption on metal atom.^{40,54,55} Our results indicated that the change of d

orbital occupancy in M/G_d is smaller than that of M/G_p after CO and H_2 adsorption. The strong adsorption of metal atom at defect point makes metal 3d electrons more localized. This reduces the number of electrons bonding with CO or H_2 . Therefore, CO and H_2 are weakly adsorbed on M/G_d .

Similar to perfect graphene, Fe/G_d , Co/G_d and Ni/G_d are the promising materials to remove CO from the H_2 feed gas, with Co/G_d slightly favored. Furthermore, the average ΔE_{diff} of M/G_d is ~ 0.42 eV lower than that of M/G_p , suggesting that M/G_p would be more efficient than M/G_d for CO and H_2 separation.

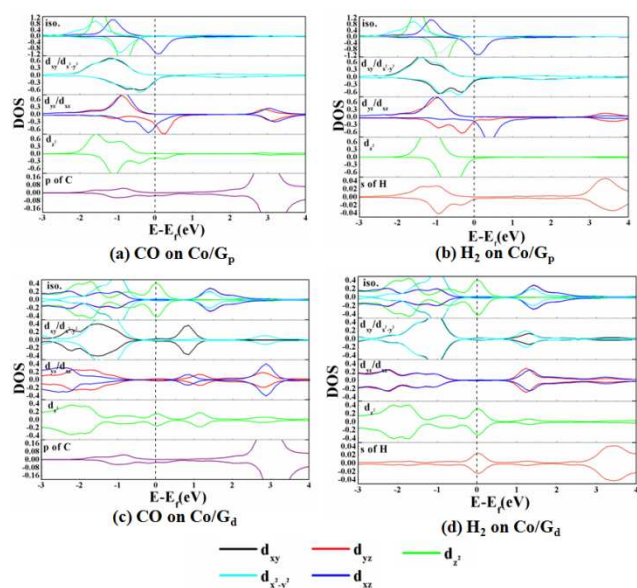


Fig. 6 (Color online) The partial density of states (DOS) of CO and H_2 adsorption on Co/G_p and Co/G_d . For detail description, see Fig. 5.

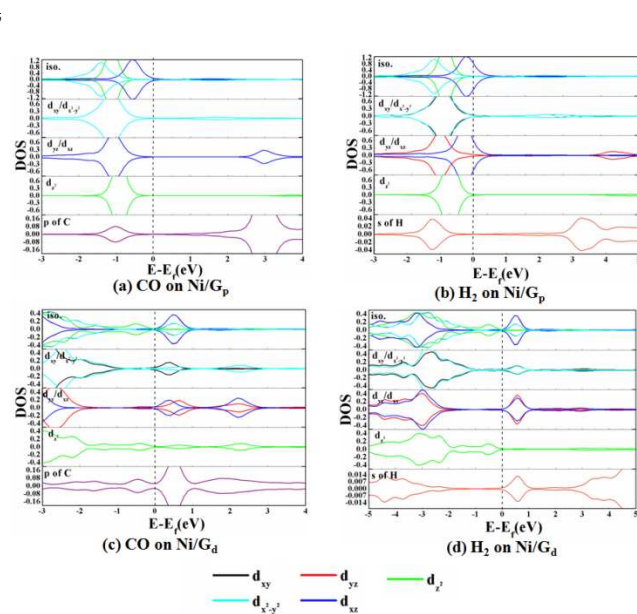


Fig. 7 (Color online) The partial density of states (DOS) of CO and H_2 adsorption on Ni/G_p and Ni/G_d . For detail description, see Fig. 5.

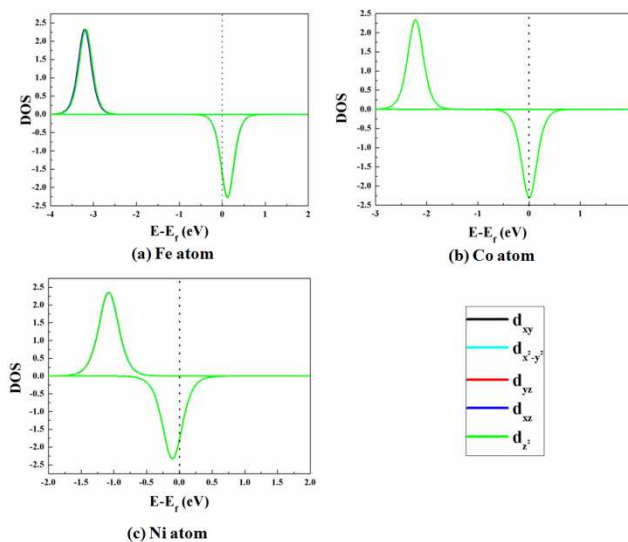


Fig. 8 (Color online) The partial density of states (DOS) of single Fe (a), Co (b) and Ni (c) atom.

3.4. The adsorption mechanism of CO/ H_2 on M/G_p and M/G_d ($M=Fe, Co$ and Ni)

According to the discussion above, it is seen that Fe, Co and Ni systems with large ΔE_{diff} are more effective to remove CO from H_2 feed gas. To further understand the mechanism of CO and H_2 adsorption on M/G_p and M/G_d ($M=Fe, Co$ and Ni), we studied their electronic structures. The partial density of states of M/G_d ($M=Fe, Co$ and Ni) are shown in Fig. 5-7, respectively. Since compared with $Fe/G_{p(d)}$, the adsorption mechanism of CO and H_2 is the same as $Co/G_{p(d)}$ and $Ni/G_{p(d)}$, only the mechanism for $Fe/G_{p(d)}$ is discussed. For $M/G_{p(d)}$ ($M=Fe, Co$ and Ni) without gas molecule adsorption (defined as iso. in Fig. 5-7), the five d orbitals of metal atoms split to three groups based on energy as (d_{yz} and d_{xz}), (d_{xy} and $d_{x^2-y^2}$), and d_{z^2} . Compared with the single metal atoms (Fig. 8), it is seen that all the orbitals of d band moves upwards and close to the Fermi level, particularly for d_{yz} and d_{xz} . This suggests that the graphene substrate enhances the adsorption of gas by increasing the d band, in agreement with d band center theory.^{54,55}

For perfect graphene, the calculated density of states of Fe/G_p indicated that only d_{yz} and d_{xz} orbitals form bonding state (below Fermi level) and anti-bonding state at ~ 3.0 eV (above Fermi level) with carbon p orbitals. For other orbitals, only bonding state is obtained (Fig. 5a). Therefore, the main contribution to CO adsorption would come from d_{yz} and d_{xz} orbitals. For H_2 adsorption, Fig. 5b shows clearly that only d_{yz} orbital form a clear bonding and anti-bonding states with the s orbital of H, suggesting that d_{yz} orbital is important in H_2 adsorption.

For defect graphene, the clear bonding and anti-bonding states are observed for all d orbitals (Fig. 5), different from the case of perfect one. This demonstrated that metal atom has stronger interaction with defect graphene, in agreement with high adsorption energy of M/G_d compared with M/G_p (Fig. 2). For CO adsorption (Fig. 5c), d_{yz} and d_{xz} orbitals have the largest energy gap between bonding and anti-bonding states. This means that these two orbitals are important for the dissociation of metal-

carbon bond and make the largest contribution to CO adsorption. Similarly, for H₂ adsorption on Fe/G_d (Fig. 5d), both d_{yz}/d_{xz} and $d_{xy}/d_{x^2-y^2}$ orbitals are important for H₂ adsorption, with the former slightly favored.

4. Conclusions

For 3d metal/perfect-graphene (M/G_p) and metal/defect-graphene (M/G_d) (M= Sc - Zn), very different behavior is observed for the adsorption of CO and H₂. The two gas molecules interact more strongly with perfect graphene (M/G_p) compared with defect one (M/G_d). For both defect and perfect graphene, CO bonds more strongly with M/G_{d(p)}, compared with H₂. Fe, Co and Ni show high efficiency in separating CO from H₂ feed gas. d_{yz} or/and d_{xz} orbitals of the metal atoms are found to play a major role in CO and H₂ adsorption. We expect that the obtained results are useful for removing CO from H₂ feed gas and reduce or eliminate the CO poisoning on anode catalysts.

Acknowledgements

This work is supported by the National Natural Science Foundation of China (Grant Nos: 21221061, 21203174), Jilin Province Youth Fund (Grant Nos: 20130522141JH) and Jilin Province Computing Center (Grant Nos: 20130101179 JC-08, 20130101179 JC-07). The authors also thank the financial support from Department of Science and Technology of Sichuan Province (Grant Nos: 2011GZX0077, 2012JZ0007, 2014HH0049). Part of the computational time is supported by the Performance Computing Center of Jilin University.

Notes

^a State Key Laboratory of Rare Earth Resource Utilization, Changchun Institute of Applied Chemistry, Chinese Academy of Sciences, Changchun 130022, P. R. China. E-mail: ywang_2012@ciac.ac.cn (YW); zjwu@ciac.ac.cn (ZJW).

^b Energy Conversion R&D Center, Central Academy of Dongfang Electric Corporation, Chengdu 611731, P. R. China; E-mail: tanghao@dongfang.com (HT)

† Electronic Supplementary Information (ESI) available: Fig. S1 and S2 give the structures of metal atom (Sc - Zn) adsorption on G_p and G_d, respectively; Fig. S3 and S4 give the structures of CO and H₂ adsorption on M/G_p, respectively; Fig. S5 and S6 give the structures of CO and H₂ adsorption on M/G_d, respectively. See DOI: 10.1039/b000000x/

References

- L. Carrette, K. A. Friedrich and U. Stimming, *Chem. Phys. Chem.*, 2000, **1**, 162-193.
- J. C. Davies, J. Bonde, Á. Logadóttir, J. K. Nørskov and I. Chorkendorff, *Fuel Cells*, 2004, **5**, 429-435.
- W. Vogel, J. Lundquist, P. Ross and P. Stonehart, *Electrochim. Acta*, 1975, **20**, 79-93.
- H. Igarashi, T. Fujino and M. Watanabe, *J. Electroanal. Chem.*, 1995, **391**, 119-123.
- M. Watanabe and S. Motoo, *J. Electroanal. Chem.*, 1975, **60**, 267-273.
- E. Christoffersen, P. Liu, A. Ruban, H. L. Skriver and J. K. Nørskov, *J. Catal.*, 2001, **199**, 123-131.
- P. Liu, J. K. Logadóttir and J. K. Nørskov, *Electrochim. Acta*, 2003, **48**, 3731-3742.
- P. N. Ross, K. Kinoshita, A. J. Scarpellino and P. Stonehart, *J. Electroanal. Chem.*, 1975, **59**, 177-189.
- T. Ioroi, N. Kitazawa, K. Yasuda, Y. Yamamoto and H. Takenaka, *J. Electrochem. Soc.*, 2000, **147**, 2018-2022.
- A. C. Garcia, V. A. Paganin and E. A. Ticianelli, *Electrochim. Acta*, 2008, **53**, 4309-4315.
- K. L. Ley, R. X. Liu, C. Pu, Q. B. Fan, N. Leyarovska, C. Segre and E. S. Smotkin, *J. Electrochem. Soc.*, 1997, **144**, 1543-1548.
- F. Colmati-Júnior, W. H. Lizcano-Valbuena, G. A. Camara, E. A. Ticianelli and E.R. Gonzalez, *J. Braz. Chem. Soc.*, 2002, **13**, 474-482.
- P. P. Lopes and E. A. Ticianelli, *J. Electroanal. Chem.*, 2010, **644**, 110-116.
- J. Kaiser, L. Colmenares, Z. Jusys, R. Mörtel, H. Bönnemann, G. Kohl, H. Modrow, J. Hormes and R. J. Behm, *Fuel Cells*, 2006, **6**, 190-202.
- M. Watanabe and S. J. Motoo, *J. Electroanal. Chem.*, 1975, **60**, 275-283.
- H. Uchida, K. Izumi and M. Watanabe, *J. Phys. Chem. B*, 2006, **110**, 21924-21930.
- D. H. Lim, D. H. Choi, W. D. Lee and H. I. Lee, *App. Catal. B-Environ.*, 2009, **89**, 484-493.
- T. C. M. Nepel, P. P. Lopes, V. A. Paganin and E. A. Ticianelli, *Electrochim. Acta*, 2013, **88**, 217-224.
- S. Mukerjee, R. C. Urian, S. J. Lee, E. A. Ticianelli and J. McBeen, *J. Electrochem. Soc.*, 2004, **151**, A1094-A1103.
- M. Watanabe, H. Igarashi and T. Fujino, *Electrochemistry*, 1999, **67**, 1194-1196.
- M. Watanabe, Y. Zhu and H. Uchida, *J. Phys. Chem. B*, 2000, **104**, 1762-1768.
- M. Watanabe, Y. Zhu, H. Igarashi and H. Uchida, *Electrochemistry*, 2000, **68**, 244-251.
- Y. Dai, Y. Liu and S. Chen, *Electrochim. Acta*, 2013, **89**, 744-748.
- H. Igarashi, T. Fujino, Y. Zhu, H. Uchida and M. Watanabe, *Phys. Chem. Chem. Phys.*, 2001, **3**, 306-314.
- S. Alayoglu, A. U. Nilekar, M. Mavrikakis and B. Eichhorn, *Nat. Mater.*, 2008, **7**, 333-338.
- J. Zhang and R. Datta, *J. Electrochem. Soc.*, 2005, **152**, A1180-A1187.
- E. D. Park, D. Lee and H. C. Lee, *Catal. Today*, 2009, **139**, 280-290.
- T. Utaka, K. Sekizawa and K. Eguchi, *Appl. Catal.*, 2000, **194-195**, 21-26.
- J. R. Ladebeck, J. P. Wagner, in Handbook of fuel cell technology, Vol. 3, edited by W. Vielstich, A. Lamm, H. A. Gasteiger, Wiley-VCH, New York, 2003, pp. 190-201.
- E. I. Santiago, M. S. Batista, E. M. Assaf and E. A. Ticianelli, *J. Electrochem. Soc.*, 2004, **151**, A944-A949.
- Y. Tanaka, T. Utaka, R. Kikuchi, K. Sasaki and K. Eguchi, *Appl. Catal.*, 2003, **238**, 11-18.
- L. Chen, A. C. Cooper, G. P. Pez and H. S. Cheng, *J. Phys. Chem. C*, 2007, **111**, 5514-5519.
- C. Zhou, J. Wu, Nie, A. R. C. Forrey, A. Tachibana and H. S. Cheng, *J. Phys. Chem. C*, 2007, **111**, 12773-12778.
- G. Papoian, J. K. Nørskov and R. Hoffmann, *J. Am. Chem. Soc.*, 2000, **122**, 4129-4144.
- K. Christmann, *Surf. Sci. Rep.*, 1988, **9**, 1-163.
- D. J. Godbey and G. A. Somorjai, *Surf. Sci.*, 1988, **204**, 301-313.
- M. T. M. Koper, T. E. Shubina and R. A. van Santen, *J. Phys. Chem. B*, 2002, **106**, 686-692.
- S. E. Mason, I. Grinberg and A. M. Rappe, *J. Phys. Chem. C*, 2008, **112**, 1963-1966.
- L. Chen, B. Chen, C. G. Zhou, J. P. Wu, R. C. Forrey and H. S. Cheng, *J. Phys. Chem. C*, 2008, **112**, 13937-13942.
- D. J. D. Durbin and C. Malardier-Jugroot, *J. Phys. Chem. C*, 2011, **115**, 808-815.
- G. Kresse and J. Furthmüller, *Comp. Mater. Sci.*, 1996, **6**, 15-50.
- G. Kresse and J. Hafner, *Phys. Rev. B*, 1993, **47**, 558-561.
- G. Kresse and J. Hafner, *Phys. Rev. B*, 1994, **49**, 14251-14269.
- G. Kresse and J. Furthmüller, *Phys. Rev. B*, 1996, **54**, 11169-11186.
- P. E. Blöchl, *Phys. Rev. B*, 1994, **50**, 17953-17979.
- G. Kresse and D. Joubert, *Phys. Rev. B*, 1999, **59**, 1758-1775.
- J. P. Perdew, K. Burke and M. Ernzerhof, *Phys. Rev. Lett.*, 1996, **77**, 3865-3868.

-
- 48 H. J. Monkhorst and J. D. Pack, *Phys. Rev. B*, 1976, **13**, 5188-5192.
- 49 S. Grimme, *J. Comput. Chem.*, 2006, **27**, 1787-1799.
- 50 S. Grimme, J. Antony, S. Ehrlich and H. Krief, *J. Chem. Phys.*, 2010, **132**, 154104.
- 51 X. J. Liu, C. Z. Wang, Y. X. Yao, W. C. Lu, M. Hupalo, M. C. Tringides and K. M. Ho, *Phys. Rev. B*, **2011**, **83**, 235441.
- 52 D. Datta, J. Li and V. B. Shenoy, *ACS Appl. Mater. Interfaces*, 2014, **6**, 1788-1795.
- 53 W. Song, M. G. Jiao, K. Li, Y. Wang and Z. J. Wu, *Chem. Phys. Lett.*,
10 2013, **588**, 203-207.
- 54 B. Hammer and J. K. Nørskov, *Surf. Sci.*, 1995, **343**, 211-220.
- 55 B. Hammer, *Top. Catal.*, 2006, **37**, 3-16.